It is important for the proposed scheme to obtain the capacitor current information because it is used for the current feedback loop as well as the proposed compensator. However, the capacitor current generally has a large ripple current and cannot be directly used for the controller. Therefore, the lowpass filter with the second-order Butterworth pole locations is used in the proposed scheme. The capacitor current is first measured using the Hall effect sensor and then filtered out through the lowpass filter represented as

$$H(s) = \frac{\omega_o^2}{s^2 + \sqrt{2}\omega_o s + \omega_o^2} \tag{10}$$

where ω_o is the cutoff frequency and set as $\omega_o = 2\pi \cdot 5000$ rad/s in the experiment.

Fig. 3 shows the experimental results of the proposed scheme under $v_o^* = 150\cos\omega^* t$, $Z_L = 30\,\Omega$ (resistive), and $\omega^* = 2\pi \cdot 60$ rad/s. It is shown in Fig. 3 that the output voltage well tracks the reference. Fig. 4 shows the steady-state performance of the controllers with and without the proposed compensator under various R and R-L loads. The load power factor is 0.8 for the R-L load. It is noted that the proposed compensator effectively reduces the steady-state error under various load conditions.

Conclusions: We have presented the effective error minimisation technique for the single-phase PWM inverter. The basic concept and implementation of the proposed compensator are presented. The performance improvement is verified from experimental results. It is, therefore, expected that the proposed technique can be used for high performance AC power supply applications.

14 May 2002
Electronics Letters Online No: 20020908
DOI: 10.1049/el:20020908

Se-Kyo Chung (*Department of Control & Instrumentation Engineering, Gyeongsang National University, 900 Gazwa-Dong, Chinju, Kyungnam 660-701, Korea*)

E-mail: skchung@nongae.gsnu.ac.kr

References

1 GOKHALE, K.P., KAWAMURA, A., and HOFT, R.G.: 'Dead beat microprocessor control of PWM inverter for sinusoidal output waveform synthesis', *IEEE Trans. Ind. Appl.*, 1987, **23**, (6), pp. 901–910
2 ABDEL-RAHIM, N.M., and QUAICOE, J.E.: 'Analysis and design of a multiple feedback loop control strategy for single-phase voltage-source UPS inverters', *IEEE Trans. Power Electron.*, 1996, **11**, (4), pp. 532–541
3 RYAN, M.J., BRUMSICKLE, W.E., and LORENZ, R.D.: 'Control topology options for single-phase UPS inverter', *IEEE Trans. Ind. Appl.*, 1997, **33**, (2), pp. 493–501
4 JUNG, S.-L., and TZOU, Y.-Y.: 'Discrete sliding-mode control of a PWM inverter for sinusoidal output waveform synthesis with optimal sliding curve', *IEEE Trans. Power Electron.*, 1996, **11**, (4), pp. 567–577

Validation of SAR interferometric phase corrections in the squinted case for DEM quality enhancement

M. Bara, P. Prats, J.J. Mallorqui and J. Lopez

The focus of this report is synthetic aperture radar (SAR) interferometric techniques for mapping applications, in the presence of possible high squint values. Theoretical and experimental analysis show the presence of limitations that are overcome by the proposed phase corrections.

Introduction: The possibility of generating digital elevation models (DEMs) from interferometric synthetic aperture radar (SAR) data acquired with airborne platforms has been widely discussed [1]. Such systems are aimed at generating height data with a precision in the order of 1 to 5 metres, which can only be achieved with an accurate knowledge of the sensor movements. The radar is normally affected by the so-called squint angle (measured from boresight), which appears as a result of strong wind conditions, turbulences, etc. In this Letter we discuss its consequences on the interferometric signal, as reported in [2], where results were presented with just one squint and with a reduced set of corner reflectors concentrated on the same range and azimuth positions. However, in this Letter we fully validate the method with several squints and a set of corner reflectors spread over the image. An experimental validation with squinted data from the DLR's E-SAR system is presented, which shows that the squinted geometry induces errors in the order of the required precisions, which can be corrected with the proposed method.

Impulse response function: An expression in zero-Doppler geometry of the impulse response function (IRF) of narrowband systems, for a target located at azimuth time $t = t_0$, and a range time τ given by $\tau_0 = 2 \cdot r_0/c$, where r_0 is the closest approach distance, takes the form [2]:

$$\begin{aligned} s_c(\tau, t) = C \cdot s_r(\tau - \tau_0) \cdot s_a\left(t - t_0 - \frac{c}{2} \cdot \frac{\tan\beta(r_0)}{v} \cdot (\tau - \tau_0)\right) \\ \cdot \exp\left[-j\frac{4\pi}{\lambda} r_0\right] \cdot \exp[j2\pi f_c(t - t_0)] \\ \cdot \exp\left[-j2\pi f_0 \cdot \left(1 - \cos\beta(r_0) - \left.\frac{\partial \Delta d(t_0, r)}{\partial r}\right|_{r=r_0}\right) \right. \\ \left. \cdot (\tau - \tau_0)\right] \end{aligned} \tag{1}$$

where f_c is the Doppler centroid which appears due to a squint angle equal to β, λ is the wavelength, f_0 the centre transmitted frequency and v is the platform forward velocity. The functions named s_r and s_a are the envelopes in range and azimuth, respectively, while C is an arbitrary complex constant. The first exponential term is that which contains the distance information, which is essential for interferometric applications. Conversely, the last two terms show a linear evolution with respect to the target position. Indeed, these phase ramps in azimuth and range only appear in the squinted case, while the ramp in range also depends on the possible motion compensation function Δd applied during processing of airborne data.

Interferometric phase bias: The fact that the IRF contains phase ramps can induce a phase bias when combining two interferometric channels. If two IRFs of the shape of (1) are cross-multiplied to form an interferogram, they are normally not perfectly co-registered since this process is directly dependent on the terrain topography. Therefore, if no DEM is known *a priori* it is possible to assume that there exists a registration error given Δr_{mis} and Δt_{mis} in range and azimuth, respectively, which is translated into the following phase bias for the zero-Doppler geometry case:

$$\phi_{bias} = \frac{4\pi}{\lambda}\left[v \cdot \sin\beta(r_0) \cdot \Delta t_{mis} - \left(1 - \cos\beta_{ef}(r_0)\right) \cdot \Delta r_{mis}\right] \tag{2}$$

where an effective squint angle has been defined to include β and the Δd derivative that appear in (1). For a single-pass system both channels can be co-registered in azimuth in a precise way, since the data take is simultaneous and Δt_{mis} can be corrected by knowing the exact positions of both antennas in this direction. The remaining error, thus, depends on the second term of (2).

Phase bias correction: An appropriate method to correct the phase bias given by (2) was shown in [2]. It is an iterative approach, based on the estimation of misregistration integrated in the geocoding step, which takes into account the possible variation of squint over range and the motion compensation term (Δd) of (2). The details of this approach can be found in [2]. Basically, the correction is applied to the distance to the slave antenna (r_2), computed from the interferometric phase, for every pixel of the interferogram located at a range position r_1 from the master antenna. It also makes use of the co-registration function (f_{coreg}), the processed squint and the motion compensation data (Δd):

$$r_{2,n+1} = r_{2,0} - \left\{r_1 - f_{coreg}(r_{2,n})\right\} \cdot \left(1 - \cos\beta_{ef}(r_{2,n})\right) \tag{3}$$

where n is the iteration number. In the following Section we present a detailed validation of this method and the previous equations by using E-SAR data.

E-SAR data for the assessment: The proposed phase corrections have been tested with data acquired on a flight over the Oberpfaffenhofen airfield, Germany, in September 1999. The measurements were made in X-band (9.6 GHz), with a bandwidth of 60 MHz and a pulse repetition frequency (PRF) of 1000 Hz. An important characteristic of the flight was its squint angle, ranging approximately from 3° at near range to 7° at far range. Moreover, the test site has deployed 10 corner reflectors, the positions of which are perfectly known, spread over different azimuth and range positions providing an excellent tool in order to verify the validity of the phase corrections described above. In Fig. 1 we show the reflectivity image of the area, with the 10 ground control points (GCP) highlighted and numbered.

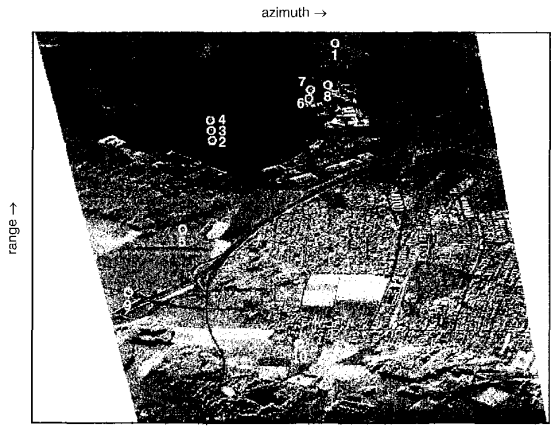

Fig. 1 *Reflectivity image of test site with 10 reflectors (Zero-Doppler geometry, processed squint = 7°)*

Processing issues: The E-SAR data in X-band is characterised by a relatively wide antenna beamwidth, designed to allow possible attitude variations during the data take. For operative focusing, a presumming step (typically of factor 4) is carried out to reduce the azimuth bandwidth. Thus, it is possible to select the azimuth band to be processed (i.e. the Doppler centroid) within a relatively wide margin. In this case the raw data lies approximately between the intervals of (−200, 800 Hz) at near range and (150, 1150 Hz) at far range. This allows one to perform a constant-squint processing with a bandwidth of $Baz = 200$ Hz centred on the frequencies between (350, 600 Hz) at any point of the swath, maintaining still reasonable SNR and ambiguity suppression.

Results of a multi-squint analysis: The data has been processed with different squint angles (from 0° to 9°), not only to prove the presence of phase errors as a result of the squint effects but also to analyse the performance of the correction method. Fig. 2 shows the result evaluated in one of the corner reflectors (no. 1) against processed squint. As can be seen, the phase error increases with the processed squint (solid line), which indicates the presence of the expected effect. In addition, it can also be observed that the proposed method is able to cancel this evolution (dotted line), leading to a phase error almost independent of the processing squint. Its mean has been chosen as the zero-value reference for the plot, since the interferometric phase requires an absolute value for calibration. An error of 20° yields a height error of ~2 m, which is in the order of the required precision. This indicates that this effect is important enough to be considered and the proposed correction is a powerful method for its cancellation. The rest of ground reflectors present the same behaviour. Fig. 3 shows the mean quadratic phase error considering all the control points for each processing squint before and after the proposed correction. For high squint values the original phase errors are quite noticeable, which gives an idea of the average impact of this effect when evaluated at different points all over the image. After the application of the phase correction method (3), the result improves to the levels given by low-squint situations. Better results are achieved with processing squints closer to the acquisition ones.

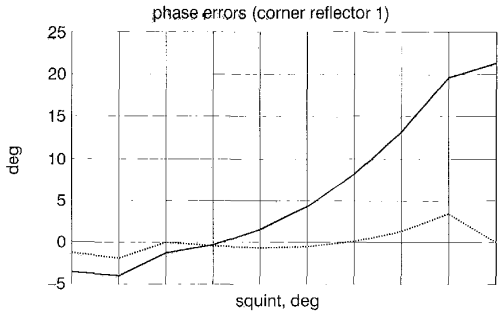

Fig. 2 *Evolution of phase error in corner reflector 1 against processed squint angle before and after proposed correction*

Conclusion: We have experimentally evaluated the analysis presented in [2], with respect to phase corrections for interferometric SAR data, in order to take into account the effects of squint, misregistration and motion compensation. We have successfully checked the theoretical expressions with squinted data from the DLR's E-SAR system. Better precision has been obtained after this phase correction according to the measurements in the ground corner reflectors. Our conclusion is that the proposed correction method allows one to obtain better quality DEMs in squinted geometries, ensuring a performance within the required specifications.

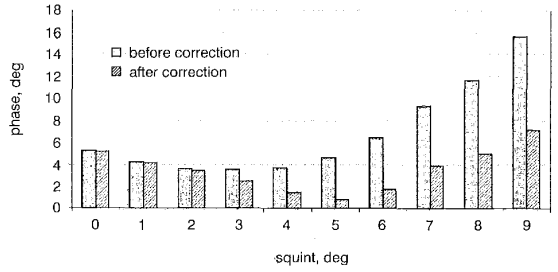

Fig. 3 *Phase error after averaging all available corner reflectors, before and after correction, against processed squint*

Acknowledgments: The authors wish to thank the German Aerospace Establishment (DLR) for supplying the E-SAR data. This work has been supported by the Spanish Commission for Science and Technology (CICYT) TIC99-1050 and the Generalitat de Catalunya 2002FI 00644.

12 August 2002
Electronics Letters Online No: 20020894
DOI: 10.1049/el:20020894

M. Bara, P. Prats, J.J. Mallorqui and J. Lopez (*Department of Signal Theory and Communications, Universitat Politècnica de Catalunya, Campus Nord, C/ Jordi Girona 1-3, E-08034 Barcelona, Spain*)

E-mail: mallorqui@tsc.upc.es

References

1 MADSEN, S.N., ZEBKER, H.A., and MARTIN, J.: 'Topographic mapping using radar interferometry: processing techniques', *IEEE Trans. Geosci. Remote Sens.*, 1993, **31**, pp. 246–256

2 BARA, M., SCHEIBER, R., BROQUETAS, A., and MOREIRA, A.: 'Interferometric SAR signal analysis in the presence of squint', *IEEE Trans. Geosci. Remote Sens.*, 2000, **38**, (5), pp. 2164–2178